Taylor & Francis
Taylor & Francis Group

Synthetic Communications

An International Journal for Rapid Communication of Synthetic Organic Chemistry

ISSN: 0039-7911 (Print) 1532-2432 (Online) Journal homepage: https://www.tandfonline.com/loi/lsyc20

# Claisen-Schmidt, aza-Michael, cyclization via cascade strategy toward microwave promoted synthesis of imidazo[2,1-b]quinazolines

Duraipandi Devi Priya & Selvaraj Mohana Roopan

**To cite this article:** Duraipandi Devi Priya & Selvaraj Mohana Roopan (2020): Claisen-Schmidt, aza-Michael, cyclization via cascade strategy toward microwave promoted synthesis of imidazo[2,1-b]quinazolines, Synthetic Communications, DOI: 10.1080/00397911.2020.1757112

**To link to this article:** https://doi.org/10.1080/00397911.2020.1757112

SYNTHETIC COMMUNICATIONS®
https://doi.org/10.1080/00397911.2020.1757112

Taylor & Francis
Taylor & Francis Group



# Claisen-Schmidt, aza-Michael, cyclization via cascade strategy toward microwave promoted synthesis of imidazo[2,1-b]quinazolines

Duraipandi Devi Priya and Selvaraj Mohana Roopan

Department of Chemistry, Chemistry of Heterocycles and Natural Product Research Laboratory, School of Advanced Science, Vellore Institute of Technology, Vellore, Tamilnadu, India

**ABSTRACT**

Imidazole blended quinazolines are having a wide run of potential applications in synthetic field. In this current investigation, we reported a modern synthesis with the help of non-conventional energy. Optimization parameters have been stabilized utilizing RSM (Response Surface Method) as well as Taguchi models. The yield obtained from the proposed protocol is significantly higher compared to other routine strategies. The products were explored by implies of $^{1}H$, $^{13}C$-NMR and HR-MS investigation. Interestingly, cyclization & aromatization has been influenced by KOH in a greater extent. It is critical that the imidazo[1,2-*b*]quinazolines show intense fluorescence emission, significant stokes shift, and high quantum yield.

**GRAPHICAL ABSTRACT**

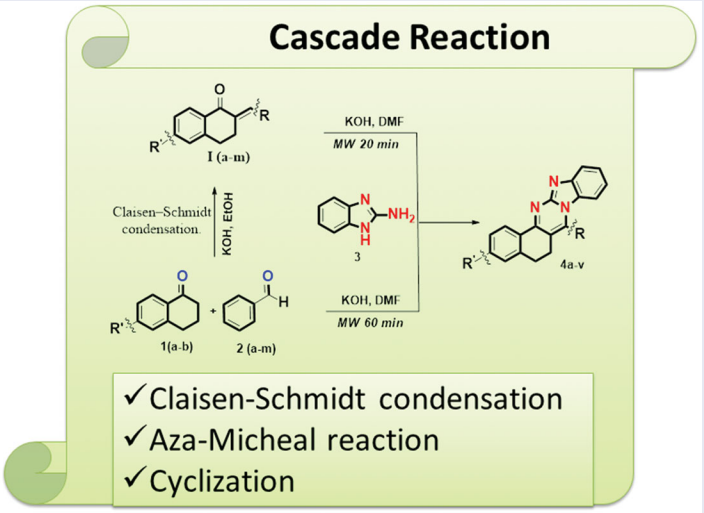


**ARTICLE HISTORY**
Received 6 November 2019

**KEYWORDS**
Fluorescence; imidazole; microwave; non-conventional; quinazoline

**CONTACT** Selvaraj Mohana Roopan mohanaroopan.s@vit.ac.in Department of Chemistry, Chemistry of Heterocycles and Natural Product Research Laboratory, School of Advanced Science, Vellore Institute of Technology, Vellore 632 014, Tamilnadu, India.

Supplemental data for this article can be accessed on the publisher's website.

## Introduction

Broadly, a heterocyclic compound that contains nitrogen within the ring exists in nature and it is imperative to human life. Imidazoles are significantly present in various parts of natural sources.[1] The biological significance of the imidazole core has been well-known in literature.[1] Among these, nitroimidazoles are being widely employed in medical care against giardial, anaerobic, amebic, and trichomonal infections.[2] The imidazoles such as Itraconazole, Ketoconazole, and Fluconazole are considered as abide medicines which will be dynamic against Leishmania.[3] However, imidazole utilize in skin therapy and visceral leishmaniasis have provided conflicting results.[4] In later a long time scientist looking for imidazole as drug that can restrain central nervous system disorders, clonidine, heart rate, phentolamine, and blood pressure.[5]Imidazole has become an important component in numerous pharmaceuticals.[6] There are many synthesized imidazoles which possess fungicides, antifungal, antiprotozoal, and antihypertensive properties.[7–10] It is also present in anticancer drug (Mercaptopurine, Tisagenlecleucel, Clofarabine) which fights leukemia.[11] The substituted imidazole derivatives were effective in the treatment of many systemic fungal infections.[12]

Quinazolines is classes of fused heterocycles, of extraordinary concern due to their biological characteristics.[13] It is used as an anti-malarial agent.[14] Many replaced derivatives of quinazoline have a broad variety of bioactivities, including antimalarial, antiviral, anticancer, anti-inflammatory, diuretic, anti-protozoan, etc.[15–20] Quinazoline and quinazolinone are too utilized within the arrangement of utilitarian functional materials for synthetic chemistry and are moreover display in multiple drug molecules such as Uroxatral, Iressa, anagrelide proquazone, biarison, afatinib, gilotrif, barasertib, dacomitinib, bunazosin, andante, gefitinib, etc.[21]

Nitrogen-bridgehead heterocyclic structures comprising an imidazole ring have an application in therapeutic and materials chemistry. These compounds have many distinct curative effects, such as antimicrobial, anticancer, anti-inflammatory, antioxidant etc.[22] The imidazo [4,5] dihydrobenzo [1,2-*c*] quinazoline ring is blending of imidazole with pharmaceutically dynamic quinazoline core as outlined in Figure 1. Moreover, these types of heterocycles are fluorescent in nature. Further, it has been used in

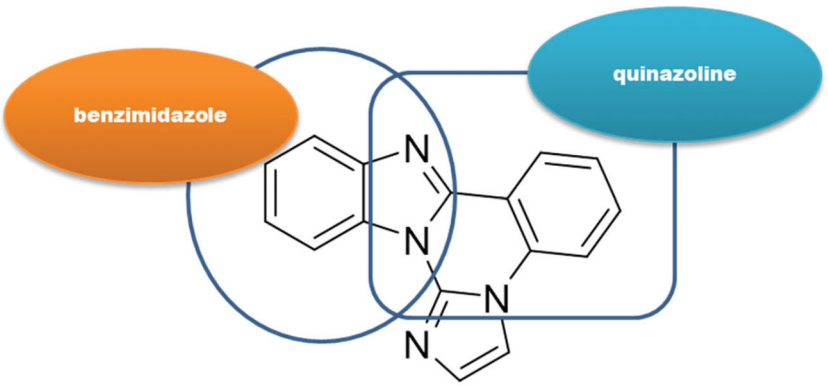


**Figure 1.** Pharmacutical importance of benzimidazole with a quinazoline.

optoelectronics, optical lasers, and organic luminophores.[23–24] Moreover, Imidazole blended quinazoline moiety has various utilization within the catalysis field.

To the leading of our information, until now, microwave advanced imidazo[2,1-*b*]quinazoline synthesis has not however detailed. From the literature review[25], we found some of the motifs were related to our synthesized compounds. The research in photoluminescence revealed that a bright blue light was emitted by all benzo [4,5]-imidazo[1,2-*c*]quinazoline compounds.[26] Synthesis of imidazo quinazolines and azole blended with pyrimido-quinazolines *via* C-N coupling/C-H functionalization was reported. The resultant compounds were exhibited interesting biological and physical properties.[27] The synthesis of imidazo-quinazolines and imidazo-quinolines *via* tandem methodology[28] are also reported. In our earlier work[29] on UV light promoted synthesis of imidazole fused quinazoline, we have faced a problem that it requires 2 h continuous light source. Thus, to overcome the disadvantages, minimization of energy, and chemicals, we made an endeavor for the basic, productive, and green way to synthesize imidazo[2,1-*b*]quinazoline utilizing one pot metal-free microwave illumination strategy. Additionally, detailed fluorescence emission properties are explored. Furthermore, here we detailed RSM (Central Composite Design/Box–Behnken Design) as well as the Taguchi models to recognize the most excellent ideal condition to synthesize imidazo[2,1-b]quinazolines.

## Results and discussion

The metal-free pathway for imidazo[2,1-*b*]quinazolines was handled by the microwave strategy utilizing DMF as a dissolvable medium within the presence of KOH (Scheme I). This reaction was carried out via both aza-Michael addition (Route-I) and cascade reaction (Route-II). During the course of study, we screened different combinations of aldehydes, amines, solvents and bases to improve the yields.

Route 1: Reaction undergoes aza-Michael addition between **I** and **3** followed by intramolecular cyclization step with the loss of water molecule (Figure 2).

Route 2: Reaction proceeds in cascade pathway i.e. first transformation is Claisen–Schmidt condensation, followed by aza-Michael addition and intramolecular cyclization step with the loss of water molecule. (Figure 2)

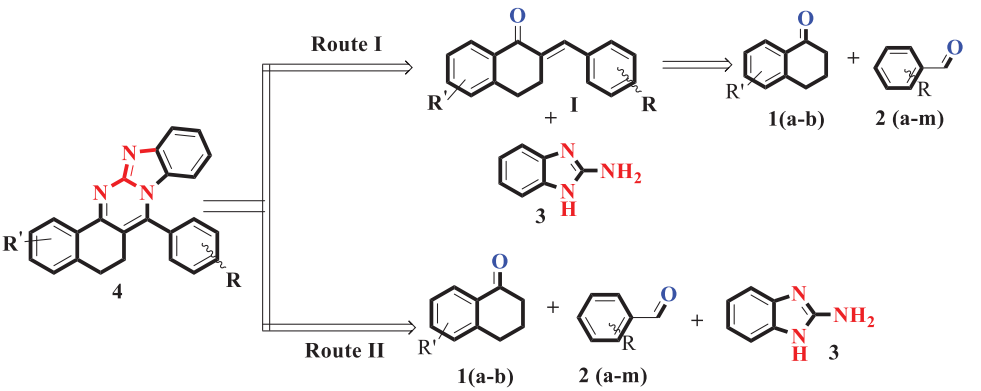


**Scheme 1.** Synthesis of imidazo[2, 1-*b*] quinazolines.

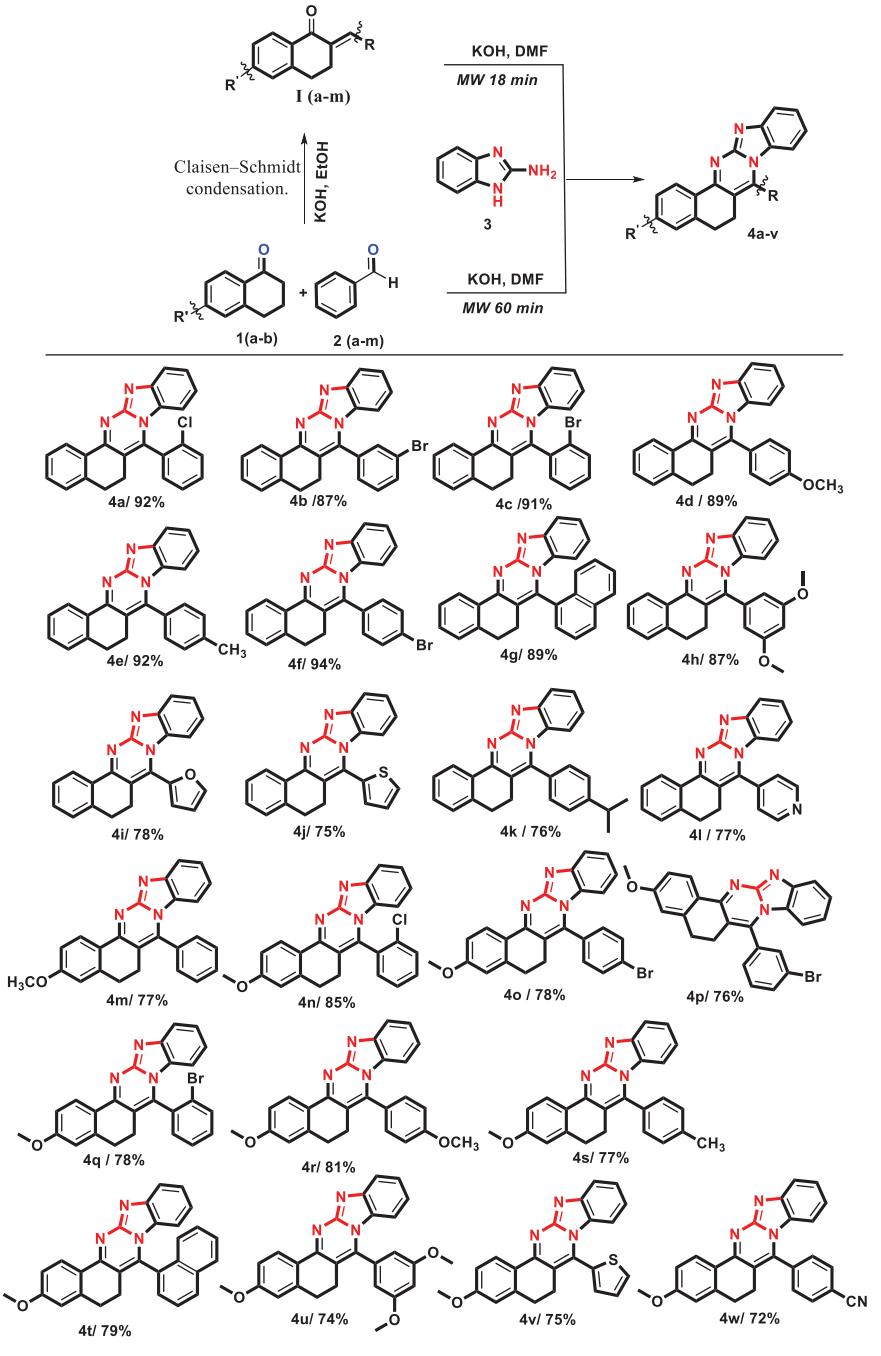


**Figure 2.** Synthesis of imidazo[2, 1-*b*] quinazolines by MW method.

Authors previously[30] reported that *β*-amino ketones were synthesized at the yield of 92% by the reaction between acetophenone, aldehyde and amine with the help of MW energy. The authors[31] utilized two step methodology and reported the synthesis of 7-amino 6*H*-benzo[c]chromen-6-ones, with 93% of yield and recently Polo et al.[32]

**Table 1.** Optimization of the reaction under, various time and temperature.

| Entry | Base | Solvent | Temperature (°C) | Source | Time (min) | [a]Yield (%) |
|---|---|---|---|---|---|---|
| 1. | – | MeOH | 60 | MW | 30 | NR |
| 2. | NaOH | MeOH | 60 | MW | 30 | 52 |
| 3. | Triethyl amine | MeOH | 60 | MW | 30 | 48 |
| 4. | pyridine | DMF | 80 | MW | 30 | 45 |
| 5. | Piperidine | DMF | 80 | MW | 30 | 61 |
| 6. | Methyl amine | DMF | 80 | MW | 30 | 31 |
| 7. | NaOMe | MeOH | 60 | MW | 30 | 53 |
| 8. | NaOEt | MeOH | 60 | MW | 30 | 44 |
| 9. | KOH | MeOH | 60 | MW | 30 | 58 |
| 10. | KOH | EtOH | 60 | MW | 30 | 76 |
| 11. | KOH | MeOH | 60 | MW | 18 | 78 |
| 12. | KOH | i-PrOH | 70 | MW | 30 | 42 |
| 13. | KOH | n-BuOH | 80 | MW | 30 | 47 |
| 14. | KOH | ACN | 80 | MW | 30 | 45 |
| 15. | KOH | THF | 80 | MW | 30 | 74 |
| 16. | KOH | DMSO | 80 | MW | 30 | 76 |
| 17. | KOH | DMF | 80 | MW | 12 | 89 |
| **18** | **KOH** | **DMF** | **80** | MW | **18** | **95** |
| 19 | KOH | DMF | 80 | MW | 25 | 95.5 |

[a]Isolated yields. The optimal conditions are shown by bold letters.

reported the synthesis of Pyrazolo-pyridines via single step approach utilizing $InCl_3$ and water with 90% yield.

At first, α, *β*-unsaturated carbonyl analogs (**Ia-v)** were prepared using the Claisen–Schmidt condensation of α-tetralone with various substituted benzaldehydes in the presence of KOH with slight modifications.[29] Subsequently, α,*β*-unsaturated carbonyl analogs were confirmed by their melting point and proton NMR. Initially, reaction between **Ia** and **3** was performed with the assistance of methanol without base which results nonappearance of **4a** (Table 1, entry 1). So we plan to introduce base NaOH in our reaction which results in 52% yield of **4a** (Table 1, entry 2). The observed yields may not be moved forward by utilizing other bases such as Triethylamine, Pyridine, Piperidine, Methylamine, NaOMe (Table 1, entries 3–8). In comparison with KOH and NaOH, better result was obtained by using KOH (10 mol-%) in the presence of DMF (Table 1, entry 9).

Response of (*E*)-2-((4-bromocyclohexa-2,4-dien-1-ylidene)methyl)-3,4-dihydronaphthalen-1(2*H*)-one (**Ia–v**) having substituted in C-4, C-3 and C-2 positions of corresponding imidazo[2,1-*b*]quinazolines comes about in 70–95% yields (Figure 2). This specific strategy was moreover successful within the case of bicyclic chalcones like 2-naphthaldehydes **4g** (89%) and **4s** (81%), and heterocyclic chalcones such as 2-thiophenyl **4j** (75%) and 2-pyridyl **4l** (76%). In spite of the fact that the yields within the final category got to be direct yields recorded in Table 1. The imidazo[2,1-*b*]quinazoline motifs were prepared by different substituted chalcones at comparable experimental conditions. The product obtained was characterized and affirmed by NMR (Nuclear Magnetic Resonance spectroscopy) and HR-MS (High-Resolution Mass Spectroscopy) analysis as displayed in Table S1. Initially, the presence of electron-donating groups such as **4–Cl, 4–Br, 4–$CH_3$** and **4–$OCH_3$** on the aromatic ring gives the corresponding product yield varying between 80 and 95% (Figure 2). The yield drop further, when the electron-donating group (–Cl) is present in C-2, C-3, C-4 position (Entries 6−15,

**Table 2.** Microwave assisted synthesis of compounds 3a–u.

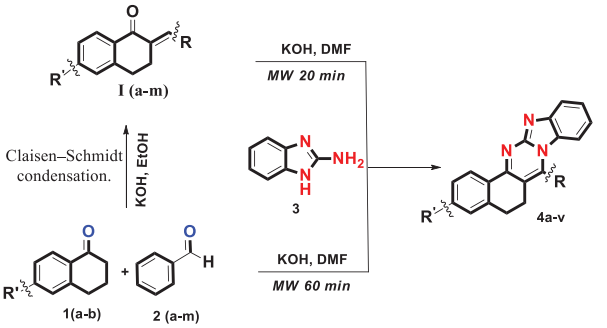


| Entry | -R | % yield | -R' | Product | HRMS (m/z) | Entry | -R | % yield | -R' | Product | HRMS (m/z) |
|---|---|---|---|---|---|---|---|---|---|---|---|
| 1 |  | 92 | -H | 4a | 381. 1033 | 12 |  | 77 | -H | 4l | 336.3890 |
| 2 |  | 87 | -H | 4b | 425.3075 | 13 |  | 85 | $-OCH_3$ | 4m | 411.8820 |
| 3 |  | 91 | -H | 4c | 425.3074 | 14 | 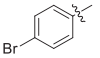 | 78 | $-OCH_3$ | 4n | 456.3332 |
| 4 | 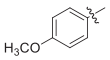 | 89 | -H | 4d | 377.4370 | 15 |  | 96 | $-OCH_3$ | 4o | 456.3332 |
| 5 |  | 92 | -H | 4e | 361.4370 | 16 |  | 78 | $-OCH_3$ | 4p | 456.3331 |
| 6 |  | 94 | -H | 4f | 425.3074 | 17 |  | 77 | $-OCH_3$ | 4q | 391.4640 |
| 7 |  | 89 | -H | 4g | 397.4702 | 18 | 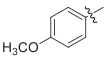 | 81 | $-OCH_3$ | 4r | 407.4631 |
| 8 |  | 87 | -H | 4h | 407.4630 | 19 |  | 79 | $-OCH_3$ | 4s | 427.4960 |
| 9 |  | 78 | -H | 4i | 337.3738 | 20 |  | 74 | $-OCH_3$ | 4t | 437.4890 |
| 10 |  | 75 | -H | 4j | 353.4390 | 21 |  | 75 | $-OCH_3$ | 4u | 383.4650 |
| 11 |  | 76 | -H | 4k | 389.4910 | 22 |  | 72 | -H | 4v | 372.4310 |

Table 2) and the excellent yield (95%, entry 12, Table 2) was attained with KOH. In most of the cases, the imidazo[2,1-*b*]quinazolines are synthesized as high purity.

Scope of the reaction was investigated with the optimized conditions. Electron deficient and rich carbonyl compounds are endured in the reaction. Electron rich substrates provide higher yields than electron-poor counterparts. The 4-pyridine carboxaldehyde results in good process; addition to this 4-bromoaldeyde also results in good yields which can be further utilized for coupling reactions.

One-pot three-component route is the alternate way to synthesis imidazo[2,1-*b*]quinazolines. As illustrated in Scheme 1, compound **1a** reacted with 2-amino benzimidazole **2a**, α-tetralone **3a** and substituted aldehydes bearing ortho, meta, and para substituents

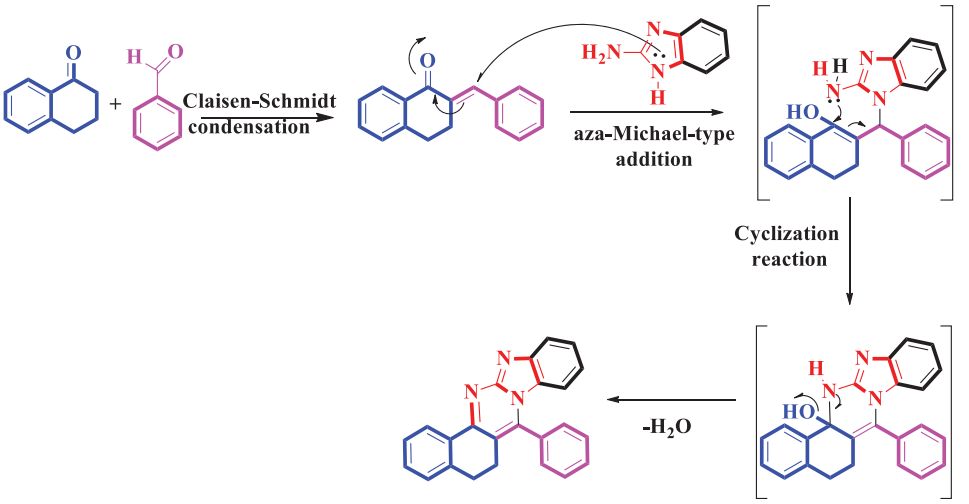


**Scheme 2.** Possible mechanism for the transformation.

on the aromatic ring to provide **4a–u** within moderate to good yields (Table 2). Electron donating group substituted aldehydes (Table 2, entries 2–6) gave better yields than withdrawing groups substituted aldehydes (Table 2, entries 7–8, 20). However, our reaction was not limited to simple aldehydes further, the imidazo[2,1-*b*]quinazoline motifs were produced by similar experimental conditions with different aldehydes and the product obtained was confirmed by NMR and HR-MS (Table S1).

## Mechanism

Mechanistically, we accept that this change is related to the imidazo[2,1-*b*]quinazolines that we have been reported previously. We proposed that the reaction proceeds by formation of α,β unsaturated ketones, via Claisen–Schmidt condensation route (Scheme 2). Further 2-aminobenzimidazole react with variety of substituted α,β unsaturated ketones to produce corresponding product via aza-Michael intermediate followed by cyclization step. Then the intermediate eliminates the water molecules to achieve **4a** as a final product.

## RSM analysis

Response surface methodology (RSM) is one of the standard methods for the optimization of the reaction parameters using Box-Behnken design (BBD)[33–35] model. Here we used this design for the microwave optimization of imidazo[2,1-*b*]quinazolines synthetic convention. The selected independent variables where base concentration, time, MW power and the yield of the synthetic analogs was a response of this model. The determined values (−1.0 + 1) of the variables are recorded in Table 3. Agreeing to the BBD second-order design; this study reveals three-level replications at the center point. Here, totally 15 runs were performed utilizing BBD, due to varieties in parameters the

**Table 3.** Coded levels for independent variables for BBD.

| Variables | Symbol | −1 | 0 | 1 |
|---|---|---|---|---|
| Base concentration (mM) | x | 2.5 | 5 | 7.5 |
| Time (min) | y | 12 | 18 | 24 |
| MW Power (W) | z | 100 | 200 | 300 |

**Table 4.** Experimental matrix and results for BBD.

| Base concentration (mM) | Time (min) | MW power W | Experimental yield (%) | Theoretical yield (%) |
|---|---|---|---|---|
| 2.5 | 18 | 100 | 57 | 58 |
| 5 | 12 | 300 | 84 | 81 |
| 7.5 | 18 | 100 | 81 | 79 |
| 7.5 | 18 | 300 | 93 | 90 |
| 7.5 | 24 | 200 | 92 | 90 |
| 5 | 12 | 100 | 78 | 75 |
| 5 | 24 | 300 | 92 | 95 |
| 2.5 | 12 | 200 | 54 | 55 |
| 5 | 24 | 100 | 82 | 84 |
| 7.5 | 12 | 200 | 83 | 86 |
| 2.5 | 24 | 200 | 79 | 74 |
| 5 | 18 | 200 | 95 | 94 |
| 5 | 18 | 200 | 94 | 94 |
| 2.5 | 18 | 300 | 64 | 65 |
| 7.5 | 18 | 200 | 91 | 92 |

obtained results were arranged in table 4. Utilizing RSM, the quadric polynomial regression equation (Y) of the yield expressed as follows,

$$Z = 94.2391 + 11.7446\ x + 5.75000\ y + 4.37500\ z - 13.9402\ x * x\ - 3.42935\ y * y - 6.67935\ z * z - 4.00000\ x * y + 1.25000\ x * z + 1.00000\ y * z \quad (1)$$

The Equation (1) represents the terms of x denotes base concentration, y denotes time, and z denotes temperature

Based on the experimental results found ANOVA table of the different variables were developed and displayed in Table 5. An ANOVA experimental result was utilized for the stability and reliability of the BBD model. If the $p$ value is less than 0.005 the model should be significant. For the first three cases it denotes the model is significant and it has more influence on the results. Figure 3 represent the fine relationship between the theoretical values and the experimental values. The $R^2$ value of the model is 96.8%; which clearly specifies that current model should be very well fits with the total error value. Another important parameter of the surface models was established utilizing ANOVA (Table 5). The $F$-value is 16.86 of the quadratic model indicated that the model was significant. The "Lack of Fit $F$-value" is 39.16, which clearly shows that the lack of fit is not significant.

## *Graphical representation of BBD model*

The synthesis parameters were investigated via 3D response surface diagrams and their corresponding 2D contour diagrams. Here the diagrams represented as interaction or relationship between yield Vs. optimized conditions. The 3D response surface graphs and its equivalent contour graphs were employed for the optimization of base

**Table 5.** ANOVA analysis of variance for yield.

| Analysis of variance for yield | | | | | | |
|---|---|---|---|---|---|---|
| Source | DF | Seq SS | Adj SS | Adj MS | *F* | *p* |
| Regression | 9 | 2392.12 | 2392.12 | 265.791 | 16.86 | 0.003 |
| Linear | 3 | 1645.51 | 1626.20 | 542.066 | 34.39 | 0.001 |
| Square | 3 | 672.36 | 672.36 | 224.121 | 14.22 | 0.007 |
| Interaction | 3 | 74.25 | 74.25 | 24.750 | 1.57 | 0.307 |
| Residual error | 5 | 78.82 | 78.82 | 15.763 | | |
| Lack-of-fit | 4 | 78.32 | 78.32 | 19.579 | 39.16 | 0.119 |
| Pure error | 1 | 0.50 | 0.50 | 0.500 | | |
| Total | 14 | 2470.93 | | | | |

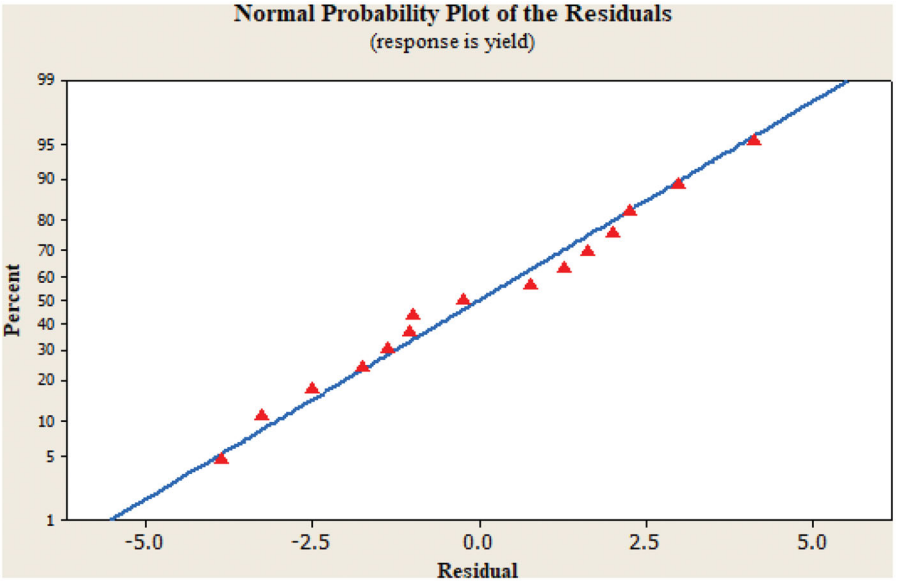


**Figure 3.** The relationship between the theoretical and experimental values.

concentration (x), time (y), MW power (z), and its plots existed in Figures 4(a–c) and 5(a–c). The influence of the base concentration (x) and time (y) explains in the Figure 4. A contour plot represent that base concentration increases the reaction convention and yield were. Figure 4b and 4c also explains the interaction between the MW Power (z) Vs. base concentration (x) and time (y) Vs MW Power (z). Here also when the power increases automatically the yield got increased, as well as when the time increases, the yield increased. The yield convention was greater than 90%. The response 3 D plots also explain the effect of interaction between the reactants. Figure 5(a–c) represents the yield variation with respect to all independent variables.

Form this observation the yield% might be increased due to the increases of, x in 5 mMol%, y in 18 min, and z in 200 W. The results clearly matched with the experimental method of imidazo[1,2-*b*]quinazoline analogs.

## *CCD design and statistical analysis*

CCD method is considered as an important design in RSM model which was also utilized to study the effect of variables. Here also, we utilized Yield as response with

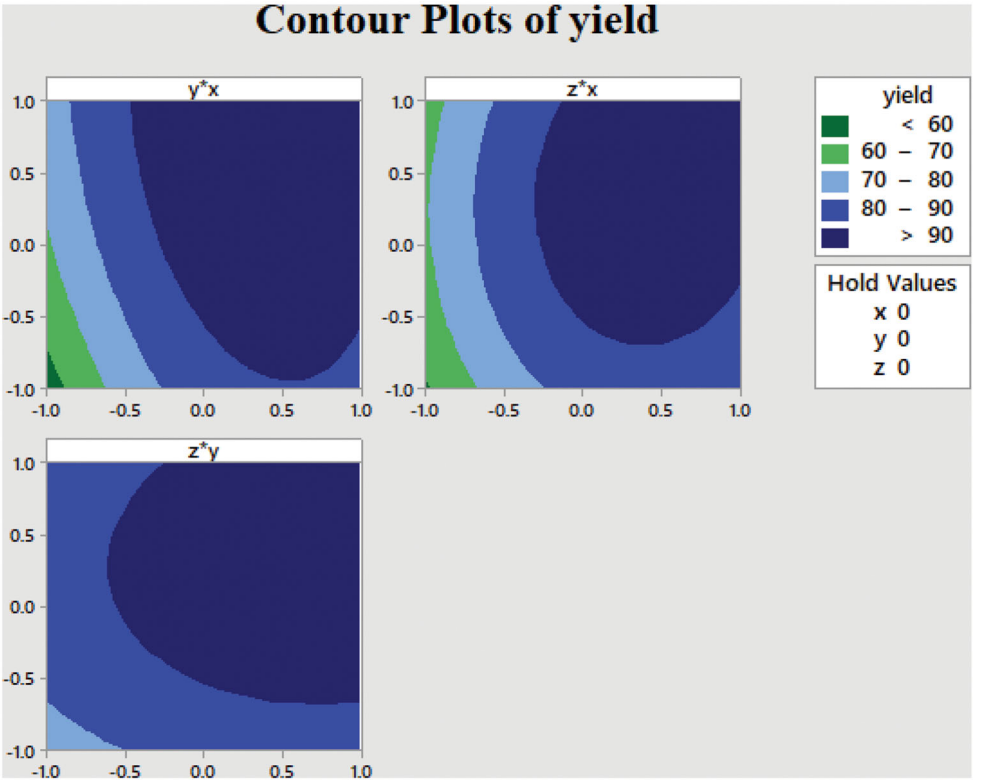


**Figure 4.** Contour plots for different parameters on the conversion of yield (%). (a) Effect of x and y. (b) Effect of z and x. (c) Effect of z and y.

respect to base concentration, time, and MW power. Table 3, denotes the range of the variables, as well as 20 experiments, which were analyzed in the CCD model (Table 6). The regression equation is as follows,

$$\text{Yield} = 94.23 + 5.200\ \text{x} + 5.900\ \text{y} + 7.500\ \text{z} - 2.37\ \text{x} * \text{x} - 9.87\ \text{y} * \text{y} - 6.87\ \text{z} * \text{z} - 1.00\ \text{x} * \text{y} - 0.50\ \text{x} * \text{z} - 1.25\ \text{y} * \text{z}$$

From this model, Table 7 illustrates the analysis of variance using Fisher's statistical analysis which was utilized to investigate the significance and capability of the model. The $F$ and $p$-value of this model 69.45 and 0, respectively implies that, it is a highly significant model. The $R^2$ value also shows that 97.36% of this model is a good statistical model.

The 3D plot and 2D contour plots represents that, corresponding interactions between base concentration (x) and time (y) fixed at MW power (z) (Figure 6A and 6B), MW power (z), base concentration (x), fixed at time (y) (Figure 6C and 6D) and time (y) and MW power (z) fixed at base concentration (x) (Figure 6E and 6F) point out that all the factors examined are interconnected.

### *Influence of base concentration (x) on product yield*

The Microwave synthesis of the imidazo[1,2-*b*]quinazoline yield was investigated by the effect of base concentration. Here the base concentration varying from 2.5 mM to

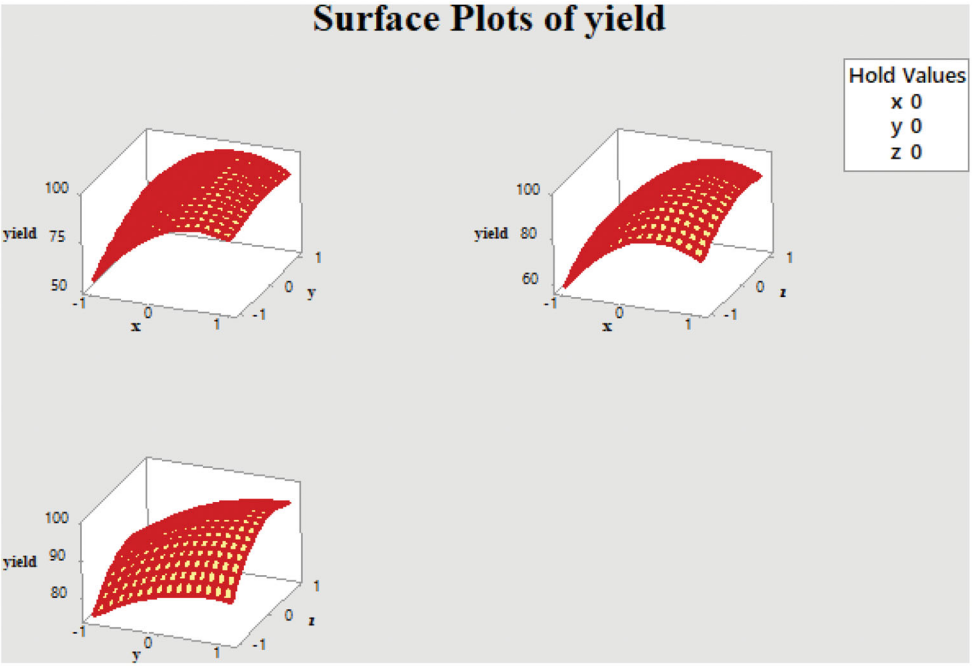


**Figure 5.** 3D surface plots for different parameters on the conversion of yield (%). (a) Effect of y and x. (b) Effect of z and x. (c) Effect of z and y.

**Table 6.** CCD matrix of the three factors in coded units along with the experimental and predicted responses.

| Std Order | RunOrder | PtType | x | y | z | Experimental yield (%) | Theoretical yield (%) |
|---|---|---|---|---|---|---|---|
| 18 | 1 | −1 | 0 | 0 | 1 | 89 | 92 |
| 13 | 2 | −1 | −1 | 0 | 0 | 85 | 83 |
| 17 | 3 | −1 | 0 | 0 | −1 | 78 | 77 |
| 16 | 4 | −1 | 0 | 1 | 0 | 86 | 87 |
| 20 | 5 | 0 | 0 | 0 | 0 | 95 | 96 |
| 15 | 6 | −1 | 0 | −1 | 0 | 75 | 75 |
| 14 | 7 | −1 | 1 | 0 | 0 | 91 | 94 |
| 19 | 8 | 0 | 0 | 0 | 0 | 95 | 91 |
| 3 | 9 | 1 | 1 | −1 | 1 | 88 | 86 |
| 5 | 10 | 0 | 0 | 0 | 0 | 95 | 96 |
| 6 | 11 | 0 | 0 | 0 | 0 | 95 | 96 |
| 1 | 12 | 1 | −1 | −1 | −1 | 56 | 56 |
| 2 | 13 | 1 | 1 | 1 | −1 | 83 | 81 |
| 4 | 14 | 1 | −1 | 1 | 1 | 87 | 86 |
| 7 | 15 | 1 | 1 | −1 | −1 | 67 | 67 |
| 11 | 16 | 0 | 0 | 0 | 0 | 95 | 94 |
| 10 | 17 | 1 | 1 | 1 | 1 | 92 | 91 |
| 12 | 18 | 0 | 0 | 0 | 0 | 95 | 94 |
| 9 | 19 | 1 | −1 | −1 | 1 | 72 | 72 |
| 8 | 20 | 1 | −1 | 1 | −1 | 69 | 70 |

7.5 mM using, different time (12–24 min) and MW (microwave) power (100–300 W) have been applied for the current synthesis method. A remarkable increase in product yield (95%) was noted at the base concentration of 5 mM. Based on these observations, the concentration of KOH (5 mM) has been thought as an appropriate condition for the reaction method.

**Table 7.** Analysis of variance for CCD model.

| Source | DF | Seq SS | Adj SS | Adj MS | *F*-value | *p*-Value |
|---|---|---|---|---|---|---|
| Model | 11 | 2386.01 | 2386.01 | 216.910 | 26.78 | 0.000 |
| Blocks | 2 | 89.97 | 77.14 | 38.571 | 4.76 | 0.043 |
| Linear | 3 | 1181.00 | 1181.00 | 393.667 | 48.61 | 0.000 |
| x | 1 | 270.40 | 270.40 | 270.400 | 33.39 | 0.000 |
| y | 1 | 348.10 | 348.10 | 348.100 | 42.98 | 0.000 |
| z | 1 | 562.50 | 562.50 | 562.500 | 69.45 | 0.000 |
| Square | 3 | 1092.54 | 1092.54 | 364.180 | 44.96 | 0.000 |
| x*x | 1 | 511.53 | 15.11 | 15.109 | 1.87 | 0.209 |
| y*y | 1 | 454.23 | 261.62 | 261.623 | 32.30 | 0.000 |
| z*z | 1 | 126.78 | 126.78 | 126.780 | 15.65 | 0.004 |
| 2-Way interaction | 3 | 22.50 | 22.50 | 7.500 | 0.93 | 0.471 |
| x*y | 1 | 8.00 | 8.00 | 8.000 | 0.99 | 0.349 |
| x*z | 1 | 2.00 | 2.00 | 2.000 | 0.25 | 0.633 |
| y*z | 1 | 12.50 | 12.50 | 12.500 | 1.54 | 0.249 |
| Error | 8 | 64.79 | 64.79 | 8.099 | | |
| Lack-of-fit | 5 | 64.79 | 64.79 | 12.959 | * | * |
| Pure error | 3 | 0.00 | 0.00 | 0.000 | | |
| Total | 19 | 2450.80 | | | | |

### *Influence of MW time (y) on product yield*

In this study, the reaction time (12–24 min) has been varied for the investigation of product yield; keeping the other independent variables (i.e.), the base concentration and MW (microwave) power as constant. The yield was improved by enhancing the time of irradiation. According to the experiment, results afford a 95% yield in 18 min of the reaction time. From the above results, 18 min irradiation time was instructed for the reaction process.

### *Influence of MW power (z) on product yield*

One of the important variables for this model is the MW power, which has been varied in order to influence the reaction yield. As a result, the product yield was increased as the MW power increased. Here, microwave power (100–300 W) was used for the optimization of yield. From all the observation, the yield of the product was maximized at 200 W of microwave power.

### *Optimization using taguchi approach*

Taguchi method[36–38] is one of the earlier statistical techniques utilized to optimize variables by a highly fractional design called an orthogonal design matrix. Compared to all the optimization methods, this method required minimum amount of data for identifying suitable reaction condition. In this model, we analyze 3 level of array which was applied for 3 different parameters. For the L9 orthogonal array, experiments were carried out to optimize the yields of the product. In common, quality loss or signal to noise (S/N) ratio (g) is utilized to speak the quality characteristics for the observed response parameters during analysis of the experimental data. In this model there are quality characteristics naming "higher is better," "smaller is better" and "nominal is better." In present study, the quality characteristic, "higher is better" was applied for the

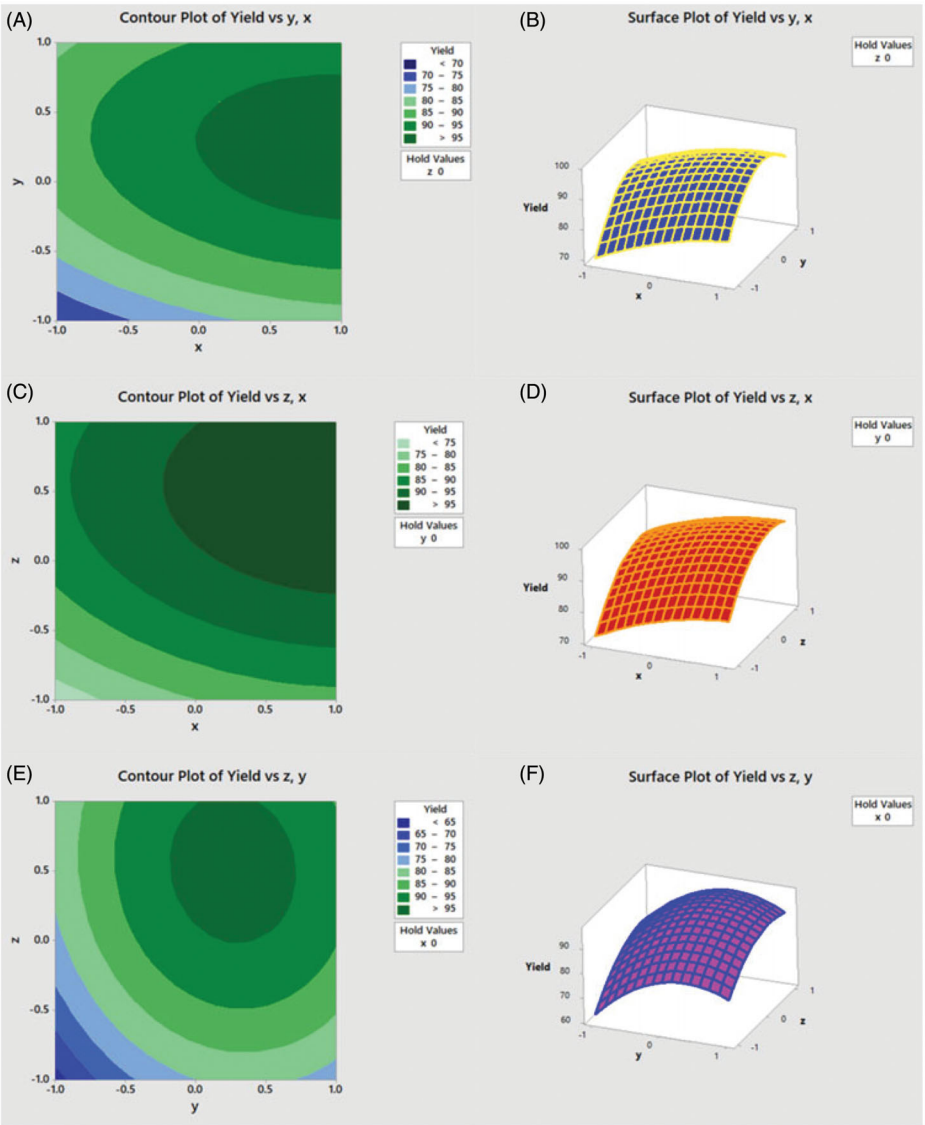


**Figure 6.** CCD/3D response surface plots and 2 D contour plots for all independent variables.

imidazo[1,2-*b*]quinazoline analogs yield. The product yield of S/N ratio is represents as eqn 2,

$$S/N = -10 \ \log_{10}\left(\sum \ (1/y^2)\right)/n \tag{2}$$

Y denotes the response, and n denotes observation of the trails.

## *S/N ratio and ANOVA*

With the L9 designed orthogonal array, the nine experiments were carried out and the product of the yield was calculated, which are given in Table 8. The synthesis of the

**Table 8.** Calculated reaction yields and their S/N ratios.

| X | y | z | Yield-1 | Yield-2 | Mean | S/N ratio |
|---|---|---|---|---|---|---|
| 2.5 | 12 | 100 | 72 | 71 | 71.5 | 36.8445 |
| 2.5 | 18 | 200 | 78 | 80 | 79.0 | 38.3997 |
| 2.5 | 24 | 300 | 84 | 82 | 83.0 | 38.1714 |
| 5.0 | 12 | 200 | 92 | 91 | 91.5 | 39.0198 |
| 5.0 | 18 | 300 | 89 | 88 | 88.5 | 38.6975 |
| 5.0 | 24 | 100 | 64 | 63 | 63.5 | 36.5039 |
| 7.5 | 12 | 300 | 86 | 89 | 87.5 | 39.2855 |
| 7.5 | 18 | 100 | 73 | 72 | 72.5 | 36.9979 |
| 7.5 | 24 | 200 | 87 | 89 | 88.0 | 38.6470 |

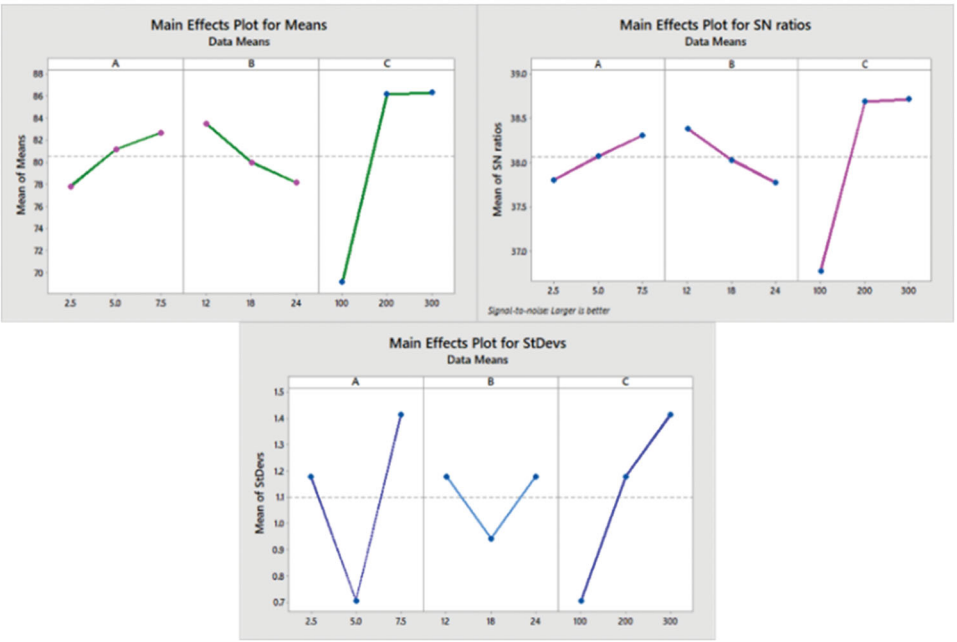


**Figure 7.** Main effects plot of design parameters through the product yield.

Imidazo[2,1-*b*]quinazolines using three optimization conditions (base concentration, reaction time and MW power) for 9 trial runs were shown in Figure 7. In this analysis, the S/N ratios for product yield are calculated using the formulae given in Equation (2).

The optimum condition of Imidazo[2,1-*b*]quinazolines yield was 92%, at 5 mM of base concentration at 12 min of reaction time, 200 W of MW power. When the base concentration increased from 2.5 to 5 mM, simultaneously the product yield increased. Also, with an increase in the reaction time and MW power product yield also increased. Figure 7 shows the plots of the main effects (i.e.) the three factors x, y and z from which the S/N ratios (larger-is-better) are calculated (obtained from Table 8). Analysis of variance is calculated for individual responses after the normalizing process of data, as shown in Table 9. As shown from the ANOVA table, the *p*-value for all variables $>0.05$ is significant.

**Table 9.** Analysis of variance for SN ratios.

| Source | DF | Seq SS | Adj SS | Adj MS | *F* | *p* |
|---|---|---|---|---|---|---|
| x | 2 | 0.3830 | 0.3830 | 0.1915 | 0.42 | 0.00704 |
| y | 2 | 0.5611 | 0.5611 | 0.2805 | 0.62 | 0.00619 |
| z | 2 | 7.3848 | 7.3848 | 3.6924 | 8.12 | 0.00110 |
| Residual error | 2 | 0.9096 | 0.9096 | 0.4548 | | |
| Total | 8 | 9.2384 | | | | |

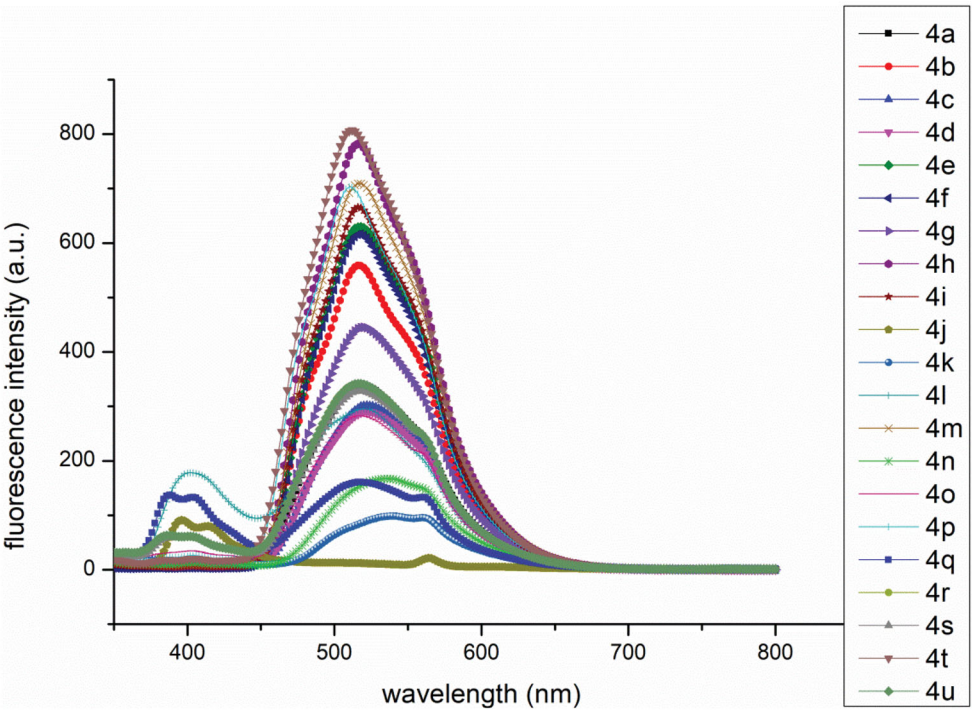


**Figure 8.** Fluorescence emission spectra of synthesized motifs.

The $R^2$ value of the S/N ratio, 90.2%, represents, the good optimum condition for multiple performance characteristics in product yield. The maximum S/N ratio is calculated to be 39.01. As a result of the MW assisted synthesis of Imidazo[2,1-*b*]quinazolines motifs, is considerably influenced by all optimum parameters.

## *Fluorescence property*

The absorption and fluorescence spectra of compounds **4a–u** were investigated via numerous solvents as illustrated in Figures 8 and 9. The absorption and emission wavelength ranges from 200 to 1200 nm. The observed absorption maxima ($\lambda_{max}$), emission maxima ($\lambda_{em}$), stokes shift and quantum yield ($\varphi$) are listed in Table 10. The values of extinction coefficient (Ɛ) were calculated from the graph of absorption vs concentration in Figure 9. Here, we used a wavelength of 350 nm for fluorescence excitation ($\lambda_{em}$). The quantum yields of synthesized motifs (**4a–u**) were decided by using tryptophan as

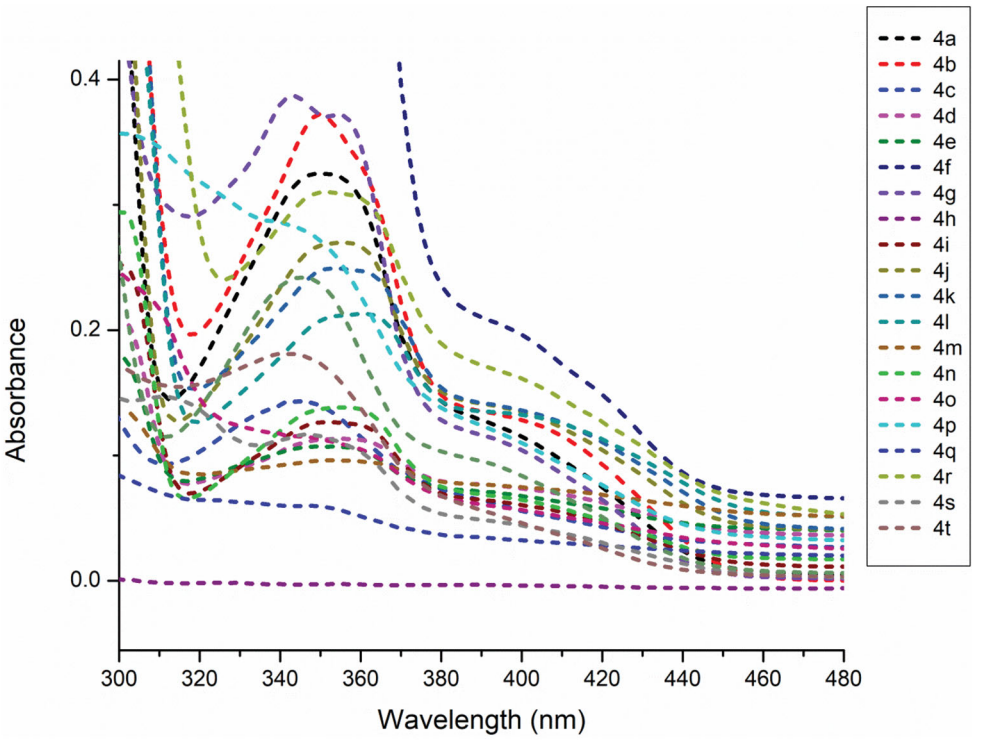


**Figure 9.** Absorption spectrum of compound **4a–s**.

**Table 10.** Photo physical properties of imidazo[2,1-*b*]quinazoline analogs.

| Entry | $\lambda max$ (abs,nm) | $\lambda max$ (em,nm) | Stokes shift (nm) | OD | $I$ | $\phi$ |
|---|---|---|---|---|---|---|
| Tryptophan | 280 | 355 | 75 | 0.384 | 158517 | 0.130 |
| **4a** | 274 | 517 | 243 | 1.0907 | 55096.09 | 0.018 |
| **4b** | 277 | 523 | 246 | 0.6356 | 34922.27 | 0.019 |
| **4c** | 277 | 521 | 244 | 0.5040 | 31938.10 | 0.022 |
| **4d** | 277 | 516 | 239 | 0.5255 | 61655.98 | 0.042 |
| **4e** | 352 | 517 | 165 | 1.142 | 58965.28 | 0.018 |
| **4f** | 278 | 518 | 240 | 1.063 | 47428.08 | 0.015 |
| **4g** | 298 | 516 | 218 | 1.316 | 7588131 | 0.020 |
| **4h** | 278 | 516 | 238 | 1.442 | 64313.04 | 0.015 |
| **4i** | 276 | 411 | 135 | 0.266 | 9093.39 | 0.012 |
| **4j** | 290 | 538 | 248 | 0.671 | 14627.76 | 0.007 |
| **4k** | 278 | 516 | 238 | 0.253 | 70773.16 | 0.100 |
| **4l** | 276 | 537 | 261 | 0.626 | 20102.08 | 0.011 |
| **4m** | 262 | 516 | 254 | 0.236 | 35284.51 | 0.058 |
| **4n** | 278 | 510 | 232 | 0.468 | 72076.15 | 0.055 |
| **4o** | 276 | 517 | 241 | 0.214 | 28383.92 | 0.047 |
| **4p** | 274 | 516 | 242 | 0.468 | 42896.68 | 0.032 |
| **4q** | 278 | 517 | 239 | 0.504 | 41788.86 | 0.029 |
| **4r** | 278 | 510 | 232 | 0.148 | 82372.39 | 0.199 |

standard. Fluorescence intensity of compounds (**4a–u**) can be justified by an effective intramolecular charge transfer (ICT). ICT explains endocyclic N acted as a donor site to donate the electrons to the aliphatic ring which turns it as an acceptor moiety. Consistently photo prompted charge exchange scheme contains a donor (D) and acceptor (A) which is coupled, which have different chromophores inside a huge

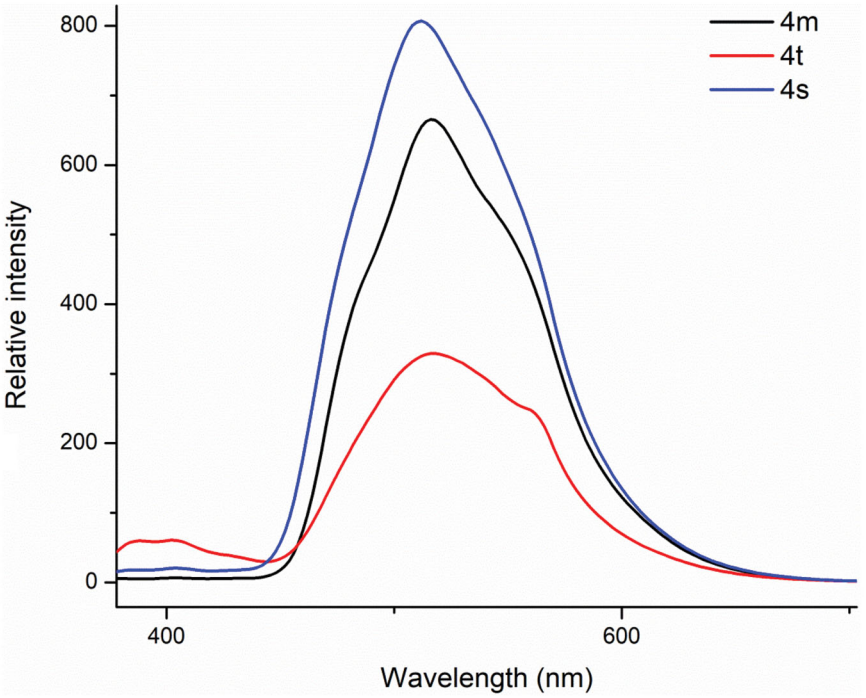


**Figure 10.** Fluorescence emission spectrum of compounds **4m, 4u, 4t**.

molecule, ruling to intramolecular charge transfer (ICT). The synthesized core motifs have less charge and ionic mesomeric structures. The shoulder peak on the left side of the emission spectra indicates two nitrogen donor atoms present in analogs which is shown in Figure 8. The motifs **4s** showed a great response to the fluorescence in the polar solvent medium. The compounds **4m**, **4u**, and **4t** showed an absorption and emission peak at 510–516 and 506–510 nm, respectively and exhibited an excellent quantum yield which is given in Figure 10. In polar solvents, synthesized compounds, **4a–u** showed a hypsochromic shift in emission spectra. Thus imidazo[2, 1-*b*]quinazoline compound may act as very good fluorophores for variety of applications in various fields.

Solvatochromism effects of compound **4a** were investigated in different solvents (Figure 11). It is portrayed in this Figure that, the absorption, as well as the emission spectra of **4a** in polar solvents, experience a redshift. High dissolvable polarity balances out the ICT excited-state molecule, which is identified with redshift of the absorption maximums which were analytically noticed.

## Experimental

### *A common technique for the production of imidazo[2,1-b]quinazoline fused heterocycles (3a–u)*

#### *Route-1*

1 mM of chalcones and 1 mM of amine were dissolved in 10 mL of DMF following with the addition of 1 mM of KOH under continuous stirring for 2 min. The reaction

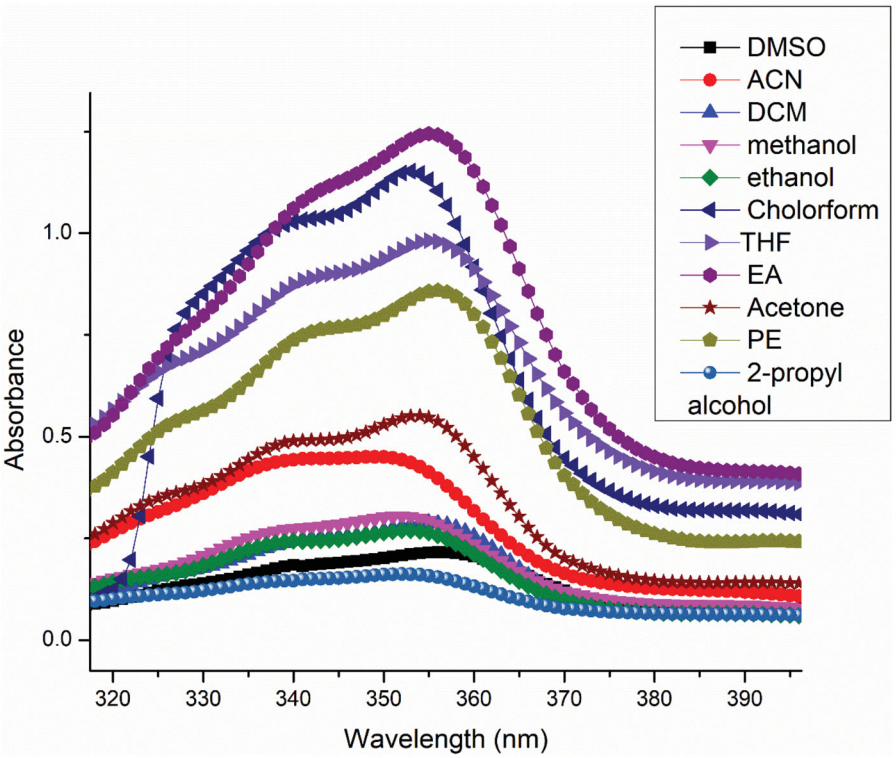


**Figure 11.** Absorption spectrum of compound 4a in various solvents.

mixture was kept it in a microwave chamber at a fixed rate for 1 min at 50 °C. From that point onward, the temperature was raised to 80 °C and kept in for 18 min. The reaction was examined by TLC, the solvent was distilled off and the residual unrefined product was purified by silica gel supported column chromatography (eluent 15–30% ethyl acetate/pet. ether).

### *Route-2*

A mixture of 2-amino benzimidazole, (1 mmol), aldehydes (1 mmol) and α-tetralone (1 mmol) were added in 5 mL of DMF followed by KOH (2.2 mmol) at room temperature. The reaction mixture was heated to 80 °C for 1 h using MW. Once the reaction is completed the reaction mixture has slowly added into ice. The product was extracted from the reaction mixture using organic solvent (ethyl acetate). To obtain the pure compound, the extract was subjected into column chromatography.

Each of the derivatives (**4a–u**) was additional verified by $^{1}$H NMR, $^{13}$C NMR, and HR-MS spectral investigations.

## *Fluorescence spectroscopy*

The absorption and emission fluorescence spectra of prepared motifs (**4a–u**) were noted down at $10^{-5}$ M concentration in ethyl acetate solvent medium. The fluorescence

spectra were recorded utilizing maximum excitation of the extensive wavelength absorption spectra. The fluorescence of the solution was estimated in a 1 $cm^3$ cuvette in right angle prearrangement. The quantum yield of the fluorescence compounds was calculated, using

$$\phi = \phi R \times I/IR \times AR/A \times \eta^2/\eta R^2 \quad (3)$$

Where $\phi R$ is standard, we are using tryptophan[19] as a reference standard, I is the area of the samples under fluorescence curve, IR is the standard curve, AR is the standard absorbance at the excitation wavelength, A is the sample absorbance at the excitation wavelength, $\eta^2$ is the refractive index of samples and $\eta R^2$ is the standard refractive index.

## Conclusions

To conclude, we have synthesized highly substituted imidazo fused quinolines using efficient microwave irradiation method under mild conditions. Here we have used various optimization methods for the synthesis parameters which were also discussed. Moreover, the product was obtained in a good amount of yield and the reaction completed within a short span of time. The synthesized analogs showed intense luminance property and possessed excellent quantum yield.

## Acknowledgments

The author thanks VIT for providing a lab facility.

## Disclosure statement

No potential conflict of interest was reported by the author(s).

## Funding

The author thanks CSIR-SRF funding provided to Devi Priya.

## References

[1] Zhang, L.; Peng, X. M.; Damu, G. L. V.; Geng, R. X.; Zhou, C. H. Comprehensive Review in Current Developments of Imidazole Based Medicinal Chemistry. *Med. Res. Rev.* **2014**, *34*, 340–437. DOI: 10.1002/med.21290.

[2] Jacqueline, A. U.; Campbell, R. W.; Benakli, K.; Upcroft, P.; Vanelle, P. Efficacy of New 5-Nitroimidazoles against Metronidazole-Susceptible and -Resistant Giardia, Trichomonas, and Entamoeba Spp. *Antimicrob. Agents Chemother.* **1999**, *43*, 73–76. DOI: 10.1128/AAC.43.1.73.

[3] Gangneux, J. P.; Dullin, M.; Sulahian, A.; Garin, Y. J. F.; Derouin, F. Experimental Evaluation of Second-Line Oral Treatments of Visceral Leishmaniasis Caused by Leishmania infantum. *Antimicrob. Agents Chemother.* **1999**, *43*, 172–174. DOI: 10.1128/AAC.43.1.172.

[4] Khalil, E. A. G.; Nur, N. M.; Zijlstra, E. E.; El Hassan, A. M.; Davidson, R. N. Failure of a Combination of Two Antifungal Drugs, Terbinafine plus Itraconazole, in Sudanese Post-Kala-Azar Dermal Leishmaniasis. *Trans. R. Soc. Trop. Med. Hyg.* **1996**, *90*, 187–188. DOI: 10.1016/S0035-9203(96)90134-0.

[5] Shallal, A. H.; Muhammed, M. A. Literature Review on the Imidazole. *International J. Multidiscip. Res. Rev.* **2019**, *5*, 1–11.

[6] Verma, A.; Joshi, S.; Singh, D. Imidazole: Having Versatile Biological Activities. *J. Org. Chem.* **2013**, *2013*, 1–329412. DOI: 10.1155/2013/329412.

[7] Bedi, P. M. S.; Kumar, V.; Mahajan, M. P. Synthesis and Biological Activity of Novel Antibacterial Quinazolines. *Bioorg. Med. Chem. Lett.* **2004**, *14*, 5211–5213. DOI: 10.1016/j.bmcl.2004.07.065.

[8] Yang, W.-C.; Li, J.; Li, J.; Chen, Q.; Yang, G.-F. Novel Synthetic Methods for N-Cyano-1H-Imidazole-4-Carboxamides and Their Fungicidal Activity. *Bioorg. Med. Chem. Lett.* **2012**, *22*, 1455–1458. DOI: 10.1016/j.bmcl.2011.11.115.

[9] Aguirre, G. 1.; Boiani, M.; Cerecetto, H.; Gerpe, A.; González, M.; Sainz, Y. F.; Denicola, A.; De Ocáriz, C. O.; Nogal, J. J.; Montero, D.; et al. Novel Antiprotozoal Products: Imidazole and Benzimidazole N-Oxide Derivatives and Related Compounds. *Arch. Pharm. Pharm. Med. Chem.* **2004**, *337*, 259–270. DOI: 10.1002/ardp.200300840.

[10] Carini, D. J.; Duncia, J. V.; Aldrich, P. E.; Chiu, A. T.; Johnson, A. L.; Pierce, M. E.; Price, W. A.; Santella, J. B.; Wells, G. J.; Wexler, R. R. Nonpeptide Angiotensin II Receptor Antagonists: The Discovery of a Series of N-(Biphenylylmethyl) Imidazoles as Potent, Orally Active Antihypertensives. *J. Med. Chem.* **1991**, *34*, 2525–2547. DOI: 10.1021/jm00112a031.

[11] Yang, J. J.; Landier, W.; Yang, W.; Liu, C.; Hageman, L.; Cheng, C.; Pei, D.; Chen, Y.; Crews, K. R.; Kornegay, N.; et al. Inherited NUDT15 Variant is a Genetic Determinant of Mercaptopurine Intolerance in Children with Acute Lymphoblastic Leukemia. *JCO.* **2015**, *33*, 1235–1242. DOI: 10.1200/JCO.2014.59.4671.

[12] Samira, I.; Patel, S.; Hasmin, M.; Patel, S. Biological Profile of Quinazoline. *Int. J. Pharm. Chem.* **2012**, *1*, 1863–1872.

[13] Singh, V. K.; Singh, S. K.; Gangwar, L. Synthesis and Antimicrobial Activity of Novel Fused 4-(3H) Quinazolinone Derivatives. *Int. J. Recent Sci. Res* **2013**, *2,* 425–428.

[14] Paul, R. G.; Cyrus, T.; Kate, E. J.; Kym, N. L.; Joan, M. C.; William, N.; Adrian, E. D.; Hayley, E. B.; Boris, P.; Sandra, D.; Jonathan, B. B.; Craig, A. H..; et al. Optimization of 2-Anilino 4-Amino Substituted Quinazolines into Potent Antimalarial Agents with Oral *in Vivo* Activity. *J. Med. Chem.* **2017**, *60*, 1171–1188.

[15] Ghorab, M. M.; Ismail, Z.; Radwan, A. A.; Abdalla, M. Synthesis and Pharmacophore Modeling of Novel Quinazolines Bearing a Biologically Active Sulfonamide Moiety. *Acta Pharmacol. Sin.* **2013**, *63*, 1–18. DOI: 10.2478/acph-2013-0006.

[16] Al-Amiery, A. A.; Kadhum, A. A. H.; Shamel, M.; Satar, M.; Khalid, Y.; Mohamad, A. B. Antioxidant and Antimicrobial Activities of Novel Quinazolinones. *Med. Chem. Res.* **2014**, *23*, 236–242. DOI: 10.1007/s00044-013-0625-1.

[17] Alagarsamy, V.; Solomon, V. R.; Dhanabal, K. Synthesis and Pharmacological Evaluation of Some 3-Phenyl-2-Substituted-3H -Quinazolin-4-One as Analgesic, Anti-Inflammatory Agents. *Bioorg. Med. Chem. Lett.* **2007**, *15*, 235–241. DOI: 10.1016/j.bmc.2006.09.065.

[18] Baba, A.; Kawamura, N.; Makino, H.; Ohta, Y.; Taketomi, S.; Sohda, T. Studies on Disease-Modifying Antirheumatic Drugs: Synthesis of Novel Quinoline and Quinazoline Derivatives and Their Anti-Inflammatory Effect. *J. Med. Chem.* **1996**, *39*, 5176–5182. DOI: 10.1021/jm9509408.

[19] Jafari, E.; Khajouei, M. R.; Hassanzadeh, F.; Hakimelahi, G. H.; Khodarahmi, G. A. Quinazolinone and Quinazoline Derivatives: Recent Structures with Potent Antimicrob. *Cytotoxic Act. Res. Pharm. Sci.* **2016**, *11*, 1–14.

[20] Rahman, M. U.; Jeyabalan, G.; Saraswat, P.; Parveen, G.; Khan, S.; Yar, M. S. Quinazolines and Anticancer Activity: A Current Perspectives. *Synth. Commun.* **2017**, *47*, 379–408. DOI: 10.1080/00397911.2016.1269926.
[21] Eryılmaz, E.; Canpolat, C. Novel Agents for the Treatment of Childhood Leukemia: An Update. *OTT*. **2017**, *10*, 3299–3306. DOI: 10.2147/OTT.S126368.
[22] Bansal, Y.; Silakari, O. The Therapeutic Journey of Benzimidazoles: A Review. *Bioorg. Med. Chem.* **2012**, *20*, 6208–6236. DOI: 10.1016/j.bmc.2012.09.013.
[23] Itoh, T. Fluorescence and Phosphorescence from Higher Excited States of Organic Molecules. *Chem. Rev.* **2012**, *112*, 4541–4568. DOI: 10.1021/cr200166m.
[24] Hirano, K.; Oderaotoshi, Y.; Minakata, S.; Komatsu, M. Unique Fluorescent Properties of 1-Aryl-3,4-Diphenylpyrido[1,2-a]Benzimidazoles. *Chem. Lett.* **2001**, *30*, 1262–1263. DOI: 10.1246/cl.2001.1262.
[25] Xie, C.; Huang, N. Y.; Ding, M. W. New Efficient Synthesis of Imidazo [2, 1-b] Quinazoline-2, 5 (1H, 3H)-Diones by a Consecutive Aza-Wittig/Heterocumulene-Mediated Annulation. *ARKIVOC*. **2009**, *10*, 220–232.
[26] Hasan, H. A.; Abdulmalek, E.; Saleh, T. A.; Rahman, A.; Basyaruddin, M.; Shaari, K. B.; Yamin, B. M.; Chan, K. W. Synthesis of Novel 6-Substituted-5,6-Dihydrobenzo[4,5] Imidazo[1,2-c] Quinazoline Compounds and Evaluation of Their Properties. **J**. Mol. Struct. **2019**, *1193*, 482–494. DOI: 10.1016/j.molstruc.2019.04.111.
[27] Chen, D.; Huang, L.; Yang, J.; Ma, J.; Zheng, Y.; Luo, Y.; Shen, Y.; Wu, J.; Feng, C.; Lv, X. Copper-Catalyzed C–N Coupling/C–H Functionalization: A Tandem Approach to Azole-Fused Quinazoline Derivatives. *Tetrahedron Lett.* **2018**, *59*, 2005–2009. DOI: 10.1016/j.tetlet.2018.04.020.
[28] Kumar, N.; Shiv, N.; Kumar, D. H.; Kumar, S. I.; Kumar, A. Synthesis of Quinazolinones, Imidazo[1,2c]Quinazolines and Imidazo[4,5c]Quinolines through Tandem Reductive Amination of Aryl Halides and Oxidative Amination of C(sp3)–H Bonds. *Eur. J. Org. Chem.* **2017**, *2017*, 514–522. DOI: 10.1002/ejoc.201601329.
[29] Devipriya, D.; Roopan, S. M. UV-Light Intervened Synthesis of Imidazo Fused Quinazoline and Its Solvatochromism, Antioxidant, Antifungal and Luminescence Properties. *J. Photochem. Photobiol. B.* **2019**, *190*, 42–49. DOI: 10.1016/j.jphotobiol.2018.11.003.
[30] Yuvaraj, P.; Kathirvelan, D.; Reddy, B. S. R. Synthesis of $\beta$-Aminoketone by Reaction of Amine and Activated Chalcone in Microwave Irradiation. *Indian J Chem B.* **2015**, *46*, 828. DOI: 10.1002/chin.201546122.
[31] Yaragorla, S.; Dada, R. Amine-Triggered Highly Facile Oxidative Benzannulation Reaction for the Synthesis of Anthranilates under Solvent-Free Calcium(II) Catalysis. *ACS Omega.* **2017**, *2*, 4859–4869. DOI: 10.1021/acsomega.7b00753.
[32] Polo, E.; Ferrer-Pertuz, K.; Trilleras, J.; Quiroga, J.; GutíErrez, M. Microwave-Assisted One-Pot Synthesis in Water of Carbonylpyrazolo[3,4-b]Pyridine Derivatives Catalyzed by $InCl_3$ and Sonochemical Assisted Condensation with Aldehydes to Obtain New Chalcone Derivatives Containing the Pyrazolopyridinic Moiety. *RSC Adv.* **2017**, *7*, 50044–50055. DOI: 10.1039/C7RA10127A.
[33] Bezerra, M. A.; Santelli, R. E.; Oliveira, E. P.; Villar, L. S.; Escaleira, L. A. Response Surface Methodology (RSM) as a Tool for Optimization in Analytical Chemistry. *Talanta.* **2008**, *76*, 965–977. DOI: 10.1016/j.talanta.2008.05.019.
[34] Mason, R. L.; Gunst, R. F.; Hess, J. L. Statistical Design and Analysis of Experiments. 2003, 1–760, ISBN: 978-0-471-37216-5.
[35] Lizotte, D. J.; Greiner, R.; Schuurmans, D. An Experimental Methodology for Response Surface Optimization Methods. *J. Glob. Optim.* **2012**, *53*, 699–736. DOI: 10.1007/s10898-011-9732-z.
[36] Ghoreishi, S. M.; Moein, P. Biodiesel Synthesis from Waste Vegetable Oil via Transesterification Reaction in Supercritical Methanol. *J. Supercrit. Fluids.* **2013**, *76*, 24–31. DOI: 10.1016/j.supflu.2013.01.011.

[37] Sivaraos, K. R.; Milkey, A. R.; Samsudin, A. K.; Dubey, P. The Mechanical Properties of Fly Ash-Based Geopolymer Concrete with Alkaline Activators. *Kidd. J. Mech. Ind. Eng.* **2014**, *8*, 35–42.

[38] Varatharajulu, M.; Jayaprakash, G.; Baskar, N.; Suresh Kumar, B. Application of RSM and Taguchi Methods for Optimizing the Transesterification of Waste Cooking Oil Catalyzed by Solid Ostrich and Chicken-Eggshell Derived CaO. *Asian J. Res. Soc. Sci. Humanit.* **2017**, *7*, 1237–1251.